



This is a repository copy of *A 2000 yr paleoearthquake record along the Conway segment of the Hope fault : implications for patterns of earthquake occurrence in northern South Island and southern North Island, New Zealand.*

White Rose Research Online URL for this paper:
<https://eprints.whiterose.ac.uk/151459/>

Version: Supplemental Material

Article:

Hatem, A.E., Dolan, J.F., Zinke, R.W. et al. (3 more authors) (2019) A 2000 yr paleoearthquake record along the Conway segment of the Hope fault : implications for patterns of earthquake occurrence in northern South Island and southern North Island, New Zealand. *Bulletin of the Seismological Society of America*, 109 (6). pp. 2216-2239. ISSN 0037-1106

<https://doi.org/10.1785/0120180313>

© 2019 Seismological Society of America. This is an author-produced version of a paper subsequently published in *Bulletin of the Seismological Society of America*. Uploaded in accordance with the publisher's self-archiving policy.

Reuse

Items deposited in White Rose Research Online are protected by copyright, with all rights reserved unless indicated otherwise. They may be downloaded and/or printed for private study, or other acts as permitted by national copyright laws. The publisher or other rights holders may allow further reproduction and re-use of the full text version. This is indicated by the licence information on the White Rose Research Online record for the item.

Takedown

If you consider content in White Rose Research Online to be in breach of UK law, please notify us by emailing eprints@whiterose.ac.uk including the URL of the record and the reason for the withdrawal request.



eprints@whiterose.ac.uk
<https://eprints.whiterose.ac.uk/>

A 2000-year paleoearthquake record along the Conway segment of the Hope fault: Implications for patterns of earthquake occurrence in northern South Island and southern North Island, New Zealand

Alexandra E. Hatem, James F. Dolan, Robert W. Zinke, Russell J. Van Dissen, Christopher M. McGuire, and Edward J. Rhodes

This electronic supplement contains seven figures and one table to aid in the understanding our arguments and data presented in the main text of this manuscript. This supplement contains high-resolution photomosaics of trench exposures, lidar topography data, offset restorations, radiocarbon age comparisons, and stratigraphic information for the GBE trench.

In Figure S1, we provide an interpreted lidar hillshade and contour (1 m) map to illustrate the origin of the shutter ridge. The topographic high at GBE, which is interpreted to be primarily a shutter ridge, and secondarily a coseismically uplifted scarp. Here, we indicate contours of specific intervals (Figure S1A). For reference, the southern end of GBE trench is located just north of the northeastern edge of the light blue 296 m closed contour. We also plotted this 296 m contour occurring east of the GBE site, across the south-flowing, steeply incised drainage.

The 296 m contour (and others) are distinctly offset by about 38 m (Figure S1B). Restoring the GBE ridge by 38 m forces this ridge to intrude into the active south-flowing drainage, indicating that the extremely steep, south-east facing incision must be younger than 38 m of displacement along the Conway segment. Restoring the GBE shutter ridge by a minimum of 38 m places the south end of our trench at the base of the alluvium/colluvium coated bedrock slope north of the trench, which provides a source for the colluvial wedges coseismically deposited.

A larger offset, ≥ 200 m, is recorded by the displacement of the thalweg this incising stream (Figure S1C). This offset places the GBE ridge well within the present-day drainage, immediately south of the steeply incised south-east facing channel wall. This restoration highlights that the origin of the GBE ridge is likely the nose of the bedrock ridge which the channel has subsequently incised.

In Figure S2, we plot high-resolution lidar data courtesy of Open Topography at the GBW site. We provide an oblique view of the trench site to highlight the steep, landslide-prone slope north of the trenches, and also to show evidence of minor-to-no channelization at the site. Contour intervals are 50 cm, and coloring represents relative elevation above sea level.

In Figure S3, we present the full trench length photomosaics of both the east and west wall of GBE. These mosaics were made using Agisoft Photoscan. Scale below east wall mosaic applies to both mosaics. On the west wall mosaic, orange spray paint numbers denote vertical string markers, and green spray paint numbers denote horizontal string markers. Note the curvature of the east wall mosaic is due to shoveling out trench spoils that were compressed into the trench wall during digging to prevent the backhoe track from sinking into the marsh.

In Figure S4, we present the full west wall of GBW T-1 photomosaic. Pink spray paint numbers represent vertical string markers, and green spray paint numbers represent horizontal string markers.

In Figure S5, we present the full exposure of the SE wall of GBW T-2. Orange numbers represent inferred-landslides (L units). Blue numbers represent paleosols (P units).

In addition to the previously discussed radiocarbon samples, we collected an additional eleven samples from the north end of the GBE trench (Figure S6). These “north marsh” samples were collected with the aim to provide a high resolution age profile throughout the marsh. Such an age profile could aid in providing limiting ages on scarp colluviation/earthquake event horizons. Such an age profile would be useful to provide this age control if the deposits were in direct, stratigraphic contact with the earthquake event horizons. However, the north marsh age profile is separated from the “south marsh” and scarp deposits by a large wood deposit. The wood mass likely acted as a depositional divide between the main marsh (north marsh) and a narrower secondary marsh (south marsh) adjacent to the scarp. Because of this physical disruption in sedimentation from north to south, we cannot use the north marsh ages to constrain events preserved in the scarp. Where possible to correlate stratigraphy across the tree, the north marsh ages are older than the south marsh ages. The material sampled from the north marsh included seeds and individual plant leaves, providing a nearly annual signal for radiocarbon determination. This observation leads us to believe that sedimentation was slower in the north

marsh compared to the south marsh, potentially due to near scarp south-ward warping of the marsh, creating a deeper depo-center in the south marsh.

In Figure 6C of the main text, we plot these 11 north marsh samples as age PDFs in an OxCal model, and have them labeled in place on SI Figure 3 on a photomosaic of the east wall of the GBE excavation. For reference, we also provide samples included in the composite GBE/GBW age model from the east wall in the scarp (yellow) and south marsh (green).

For comparison, we include calibrated radiocarbon age PDFs in Figure S6, which shows the GBE east wall. In the top left plot, we show that samples SF-6 and -48 from the north marsh are >400 years older than sample SF-40 in the south marsh. We also plot results from SF-15 and -16 of the scarp deposits, which are stratigraphically above SF-40. SF-15 and -16 are younger than SF-40, as would be expected by stratigraphic order. Because SF-6 and -48 are at nearly the same stratigraphic level as SF-15 and -16, yet are nearly 800 years older than SF-15 and -16, we cannot correlate ages of seemingly similar stratigraphic horizons from the north marsh, across the tree, to the south marsh and therefore to the scarp.

While the north marsh ages collected provided a calibrated age profile in perfect stratigraphic order (Figure 6C main text; Table 1 main text), we cannot include these results in our final age model. We prefer including ages that are in direct stratigraphic contact with other dated layers, including the south marsh samples.

In Figure S7, we present, with other data discussed in the main text, an alternative method for arriving at a combined age for GBE and GBW paleoearthquakes. This method takes the average of 10,000 randomly selected points from a given GBE and GBW probability density function, plots the results as a histogram with 15 bins, and then fits a kernel density estimation to the histogram. This results of this alternative method are plotted with the GBE probability density function, the GBW probability density function, and the OxCal combine GBE and GBW age for events 1-3 (the events which have pre- and post-date information from the GBW excavations).

In Table S1, we present abbreviated unit descriptions of all layers logged in Figure 3, with additional event related information for each unit, in Table 1. For additional unit information, we direct the reader to the main text.

List of Table Captions

Table 1: Stratigraphic information of GBE

List of Figure Captions

Figure 1: Origin of shutter ridge & other restorations

Figure 2: Oblique view of GBW topography

Figure 3: Complete GBE photomosaics

Figure 4: GBW T-1 photomosaic

Figure 5: GBW T-2 photomosaic

Figure 6: Comparison of North Marsh ages with South Marsh and Scarp ages

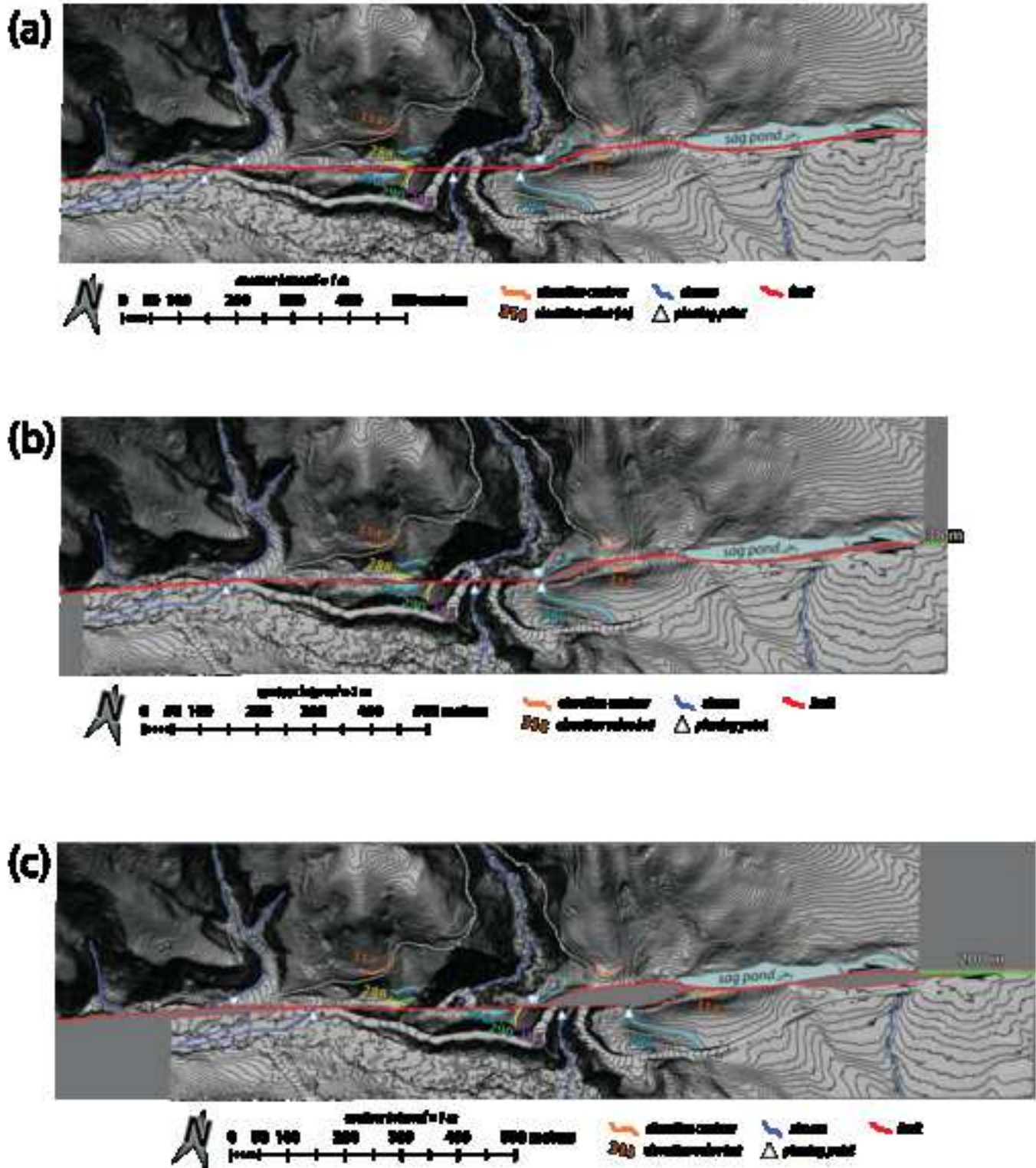
Figure 7: Comparison of GBE and GBW ages for events 1-3, including new averaging method

SI Table 1. Stratigraphic information of GBE trench

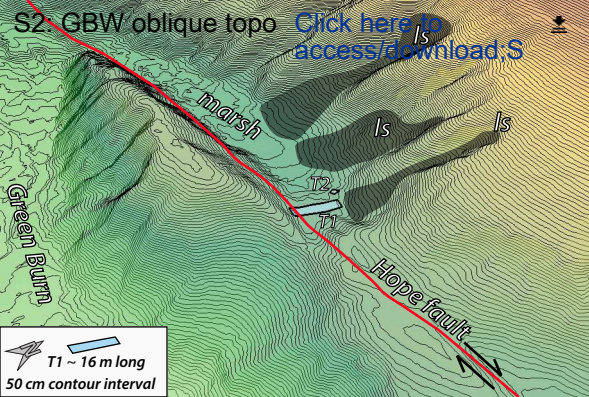
Unit label	Full unit name	Brief description	Event related deformation
A	A Horizon/active soil	Light brown, friable, relatively clast free, abundant rootlets	No rupture since soil accumulation (undeformed)
CW1	colluvial wedge 1	Dark-black to brown-gray sil to med grain sand pebbly gravel; subrounded to sub-angular clasts; matrix supported distal from scarp	deposited in GB1
CW2	colluvial wedge 2	"Hokey Pokey"/weathered orange med sand to clay clasts (saprolite?) (atypical cw observation) + subrounded to subangular clasts of Torlesse (typical cw observation); clast supported; dark black to light gray matrix of fine sand to silt	deposited in GB2
CW3a	colluvial wedge 3 intermediary	clayey silt, matrix supported, with sub-angular to sub-rounded pebbles to cobbles (~5 cm), some oxidation, bright tan to orange matrix, with stone line at base	deposited in GB3
CW3	colluvial wedge 3	numerous large (8-10 cm) sub-angular cobbles within a gray-pale brown med sand to silt/clay matrix	deposited in GB3
CW4a	colluvial wedge finer	similar to CW4 except far more matrix supported and paler in color	deposited in GB4
CW4	colluvial wedge 4	pebble to cobble deposit (max clast c. 12cm) med sand to silt matrix, sub-angular clasts, dark brown to clay matrix	deposited in GB4
CW5	colluvial wedge 5	pebble to cobble deposit; med brown, fine grained sand to silt matrix	deposited in GB5
CW6	colluvial wedge 6	moderately sorted, small pebble (mostly c. 1cm), sub-rounded, gray clay to silt	Likely deposited in older event for which we have no primary evidence of

M1	hairy peat 1	dense, black to dark brown, organic rich, massive, clay to silt, relatively dry, "proto peat"	accumulated consistently from GB3 to present
M2	organic rich silt 2	"hairy peat" relatively wet (retained water) with collapse sedge mats, organic rich, dark-brown to black, some roots	accumulated from GB3 to GB2
M3	hairy peat 3	similar to M3, with lighter brown color and more organics (more plant matter) and less matrix density (more pore water)	accumulated between GB4 and GB3
M4	organic rich silt/clay 4	light brown-gray, dense, massive, clay. Viscous fluid with slow relaxation time	accumulated between GB4 and GB3
M5	hairy peat 5	similar to M4 but with more silt and less clay (less sticky)	accumulated between GB5 and GB4
M6	organic rich silt/clay 6	dark brown to black, clay to silt, organic rich	accumulated before GB5
M7	organic rich silt/clay 7	same as M4	accumulated before GB5
B1	basal clay 1	bright tan/orange silt to clay, massive with some vertical shear fabric, rare subangular clasts (~8 cm)	pre-dates all events
B2	basal clay 2	muted tan to brown (more gray than B1), silty clay with occasional peat stringers (~5-10 cm thick)	pre-dates all events
B2'	basal clay 2 pebbly	transition between B2 and B1, appearance and shear of B2, but pebble contact of B1	pre-dates all events
B3	basal clay 3	"bedrock" dark gray to brown, dense, massive, clay. Grades to more brown + sand towards the surface, nearly no sand at trench base; potentially sheared Torlesse bedrock in situ	pre-dates all events
nM1	organic rich silt	Silt with fine grained sand; potentially a paleosol; hard and dry; dark brown to black	

nM2	“hairy peat”	Layers of compressed sedges/marsh grasses; very densely packed; retained much water; dark brown to black	
nM3	organic rich silt	Wet; dark brown; silt with abundant organics (color)	Deposited after/during possible GB6
nM4	“hairy peat”	Layers of compressed sedges/marsh grasses; very densely packed; retained much water; dark brown to black; contains chunks of wood in places	
nM5	peat	Similar to hairy peat but with less compressed grass material; black; thinly bedded	
nM6	clay	Blue-gray clay; clast free; wet	



S2: GBW oblique topo [Click here to access/download;S](#)



  T1 ~ 16 m long
50 cm contour interval



S

N

GBW T-1 West Wall

1 meter
1 meter



GBW T-2 SE Wall

1 meter

